(10) Schulz, D. N.; Sanda, J. C.; Willoughby, B. G. *ACS Symp. Ser.* **1981**, *166*, 427.
(11) Dickstein, W. H.; Lillya, C. P. *Macromolecules* **1989**, *22*, preceding paper in this issue.
(12) Hadjichristidis, N.; Fetters, L. J. *Macromolecules* **1980**, *13*, 191.
(13) Hadjichristidis, N.; Guyot, A.; Fetters, L. J. *Macromolecules* **1978**, *11*, 668.
(14) Hadjichristidis, N.; Roovers, J. E. L. *J. Polym. Sci., Phys. Ed.* **1974**, *12*, 2521.
(15) Hirshfield, S. M. U.S. Patent 3,755,283, 1971.
(16) Zelinski, R. P.; Wofford, C. F. *J. Polym. Sci., A-1* **1965**, *3*, 93.

Spin-Label-Induced Selective ^{13}C Nuclear Relaxation: Structures of the γ-Cyclodextrin–Tempone and α-Cyclodextrin–Di-*tert*-butyl Nitroxide Inclusion Complexes in Solution

Michael P. Eastman,*,† James R. Brainard,*,‡ David Stewart,§ Greg Anderson,§ and W. D. Lloyd§

Department of Chemistry, Northern Arizona University, Flagstaff, Arizona 86011, Isotope and Structural Chemistry Group, INC-4, MS-C345, Los Alamos National Laboratory, Los Alamos, New Mexico 87545, and Department of Chemistry, University of Texas at El Paso, El Paso, Texas 79968. *Received December 27, 1988*

ABSTRACT: The relative positions of the guest molecules in the γ-cyclodextrin–Tempone and the α-cyclodextrin–di-*tert*-butyl nitroxide inclusion complexes have been determined from spin-label-induced ^{13}C nuclear relaxation rates. The structures of the complexes are consistent with the sizes of the nitroxide guests relative to the hydrophobic cavity of the cyclodextrins and with the thermodynamics of complex formation. Selective proton-decoupled ^{13}C spectra demonstrate that the assignments of C2 and C5 are reversed in γ-cyclodextrin relative to α- and β-cyclodextrins.

Cyclodextrins (CDs[1]) are α-1,4-linked cyclic oligomers of D-glucopyranose that form inclusion complexes with a variety of small molecules.[2] The structure of α-CD is shown in Figure 1. Interest in the properties of these complexes has been stimulated by their suitability as model systems for probing the physical and chemical basis of molecular recognition. CDs are water soluble, have a hydrophobic cavity for specific binding of substrates, and either have catalytic groups or have sites for the introduction of such catalytic groups. Consequently, one of the most interesting applications of CDs is as simple model enzyme systems for physical and chemical study.[3] In addition, the CDs have intriguing practical applications as solubilizing agents for drug delivery and as selective reagents in extractions and separations.[4]

An important step toward understanding the forces responsible for formation of CD inclusion complexes is characterizing the structure and dynamics of the complexes in solution. Magnetic resonance spectroscopies have been applied successfully to study both structure and dynamics in a variety of CD complexes.[5] The majority of ESR studies have focused on complexes between β-CD and nitroxide-free radicals because nitroxides complexed by this molecule exhibit significant changes in g values and hyperfine splitting constants compared to uncomplexed radicals. Complexes formed between nitroxides and either α-CD or γ-CD have received relatively little attention because the changes in the ESR spectra that accompany complexation are relatively small. However, one of us (M.P.E.) has recently shown that Heisenberg exchange rates can be used to determine the thermodynamics and kinetics of α-CD and γ-CD complex formation with nitroxides;[6] this has expanded the number of CD–nitroxide complexes that can be studied by ESR.

NMR spectroscopy has been widely used for the study of CDs in both the solution and solid state. Several studies have used cross relaxation and chemical shifts to determine geometries and location of substrates in the CD cavity.[7] A potentially powerful technique that has not been widely used in studying CD complexes is paramagnetically induced relaxation of nuclear spins. This technique, introduced by Mildvan and co-workers,[8] has been used advantageously for the study of macromolecular systems. In favorable cases, it has provided a very detailed picture of the structure and dynamics of bimolecular and trimolecular complexes of enzymes with a variety of substrates and cofactors. To our knowledge, only two reports using this technique on CD complexes have appeared.[9] Ohara and Kobayashi observed the effects of several nitroxides on the ^1H spectra and ^1H T_1s of β-CD and showed that some resonances were selectively relaxed by the nitroxides. However, the results were not quantitatively analyzed to provide details on the position of the nitroxide in the inclusion complex because the ^1H spectra are poorly resolved. Although the effects of paramagnetic molecules on ^{13}C relaxation rates are smaller than their effects on ^1H relaxation rates, the effects are readily detectable, and the greater resolution of ^{13}C spectra make this nucleus an attractive probe for macromolecular systems.[10] This paper reports the effects of nitroxide-induced relaxation on the ^{13}C relaxation rates of nitroxide–CD inclusion complexes and shows that this method gives direct measures of the positions of the nitroxide substrates in the inclusion complex.

Experimental Methods

α-CD and γ-CD were purchased from Advanced Separation Technologies, Inc., Whippany, NJ, and used as received. The proton and carbon NMR spectra were consistent with the absence of any impurities. Tempone and di-*tert*-butyl nitroxide (DTBN) were purchased from Aldrich Chemical Co. Sodium ascorbate was obtained from Sigma. Solutions for NMR analysis were prepared by dissolving 50–100 mM of CD in 2.5 mL of degassed 20% or 99% D_2O/H_2O and adjusting the pH to between 6.8–7.8 with HCl and NaOH. Reported pH values are uncorrected pH meter readings. The concentration dependence of the nuclear relaxation rates was determined by titrating aliquots (10–40 μL)

† Northern Arizona University.
‡ Los Alamos National Laboratory.
§ University of Texas at El Paso.

0024-9297/89/2222-3888$01.50/0

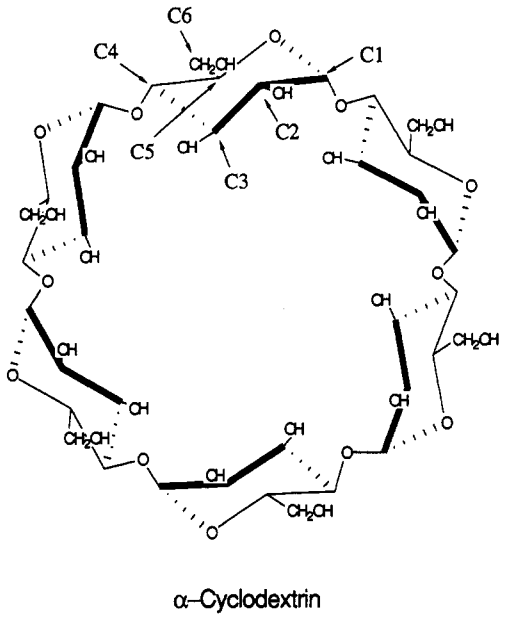

Figure 1. Structure of α-CD with the carbon atoms of the glucosyl residues numbered.

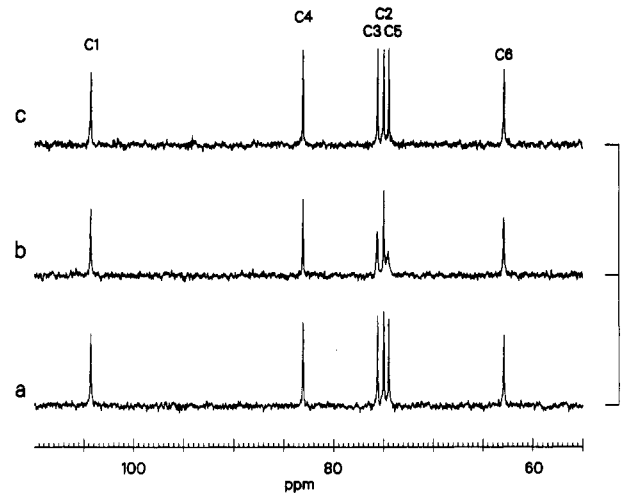

Figure 2. Proton-decoupled ^{13}C NMR spectra of (a) γ-CD, (b) γ-CD–Tempone inclusion complex, and (c) γ-CD–reduced Tempone inclusion complex.

of freshly prepared solutions of nitroxides into the CD solutions. ^1H COSY spectra for assignments were obtained on a Bruker WM300, and selective proton-decoupled carbon spectra were obtained on an IBM/Bruker AF250 pulsed NMR spectrometer. Chemical shifts were referenced to internal TSP and are judged accurate to 0.008 ppm, on the basis of the digital resolution of the spectra and the reproducibility between identical samples. All relaxation measurements were performed on the WM300 at 298 K. Spin–lattice relaxation times were determined by inversion–recovery pulse sequences using 15 τ values and delay times greater than $5T_1$. The intensities of the apodized (line broadening = 5 Hz), transformed, and normalized spectra were fit to exponential curves by using three parameters by DISNMR[12] software. In all cases, the standard deviations reported by the software were less than 7% of the T_1 values.

γ-Cyclodextrin–Tempone Inclusion Complex

The effects of 2,2,6,6-tetramethyl-4-oxopiperidinyl-1-oxy (Tempone) on the ^{13}C spectra of γ-CD in D_2O are shown in Figure 2. Figure 2a is the spectrum of 15 mM γ-cyclodextrin in D_2O, pH 7.09. The carbon assignments for C1, C4, and C6 were based on the assignments reported in the literature for α- and β-CDs.[12] The carbon numbering scheme for the glucosyl residues is shown in Figure 1. The carbon assignments were verified and carbon assignments

Table I
Chemical Shifts (δ) and Spin–Lattice Relaxation Times (T_1) for γ-CD–Tempone Complexes

	C1	C2	C3	C4	C5	C6
δ free γ-CD	104.361	75.029	75.650	83.100	74.528	62.901
δ Tempone–γ-CD complex	104.380	75.030	75.696	83.113	74.591	62.929
δ reduced complex	104.366	75.028	75.633	83.131	74.500	62.903
T_1 free γ-CD	0.174	0.187	0.188	0.185	0.184	0.107
T_1 reduced complex	0.178	0.191	0.193	0.189	0.184	0.107

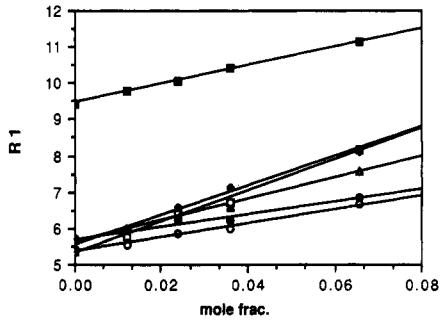

Figure 3. Effects of Tempone on the spin–lattice relaxation rates ($R1$) of carbon nuclei in γ-CD. Spin–lattice relaxation rates are plotted as a function of the mole fraction of γ-CD present in the γ-CD–Tempone inclusion complex: (●) C1; (○) C2; (□) C3; (△) C4; (◐) C5; (■) C6.

for C2, C3, and C5 were made on the basis of 2D ^1H COSY spectra[13] and selective proton-decoupled carbon spectra. Notably, the relative positions of the resonances from C2 and C5 are reversed in γ-CD relative to α-CD and β-CD. Figure 2b shows the ^{13}C spectrum of γ-CD after addition of 0.4 mM Tempone to the solution; Figure 2c shows the spectrum of the complex after reduction of the nitroxide with 0.8 mM ascorbate. The selective effects of the nitroxide on the ^{13}C line widths are readily apparent. The resonances from C3 and C5 of γ-CD are most broadened by the nitroxide, and reduction of the nitroxide reverses the broadening. Chemical shifts for the free γ-CD, γ-CD in the presence of Tempone, and γ-CD in the presence of reduced Tempone are given in Table I. Although all of the carbons give small shifts upon complexation with nitroxide, the largest shifts are observed for carbons C3 (0.04–0.06 ppm) and C5 (0.07–0.10 ppm). The small shifts observed for all of the carbon nuclei suggest that pseudocontact shifts are contributing to the line widths of resonances in the γ-CD–nitroxide complex.

In order to quantitatively measure the selective effects of nitroxide inclusion on the relaxation of ^{13}C resonances of γ-CD, spin–lattice relaxation rates were determined as a function of Tempone concentration. To facilitate the interpretation of these results in terms of the structure of the complex, the spin–lattice relaxation rates were plotted as a function of the fraction of γ-CD present in the complex. Mole fractions of complexed γ-CD were calculated from the K_a determined from ESR measurements.[6] Figure 3 shows the linear dependences of the relaxation rates of γ-CD resonances on the mole fraction of γ-CD complexed by Tempone.

The observed spin–lattice relaxation rates for a CD nucleus in the presence of an exchanging nitroxide are given by[14]

$$T_1^{-1}{}_{obs} = T_1^{-1}{}_d + f_m q/(T_{1m} + \tau_m) + 1/T_{1os} \quad (1)$$

where $T_1^{-1}{}_d$ is the diamagnetic contribution to the relaxation rate, f_m is the mole fraction of CD molecules complexing nitroxide, q is the stoichiometry of the nitroxide–

Table II
$T_1^{-1}{}_m$ and $\langle r \rangle_{rel}$ for γ-CD–Tempone Complexes

	C1	C2	C3	C4	C5	C6
$T_1^{-1}{}_m$	17.61	19.83	42.49	29.22	40.45	25.85
$\langle r \rangle_{rel}$	1.16	1.14	1.00	1.06	1.01	1.09

CD complex, T_{1m}^{-1} is the paramagnetic relaxation rate for the nucleus in the nitroxide–CD complex, τ_m is the lifetime of the nitroxide–CD complex, and $1/T_{1os}$ is the relaxation rate from outer-sphere mechanisms. The stoichiometry of the γ-CD–Tempone complex is 1:1,[6] consequently q = 1. In addition, outer-sphere mechanisms for this complex under these conditions are expected to be negligible.[14] Finally, if the lifetime of the complex, τ_m, is much shorter than the relaxation time T_{1m}, then $T_{1m} + \tau_m \sim T_{1m}$ and eq 1 can be simplified to

$$T_1^{-1}{}_{obsd} = T_1^{-1}{}_d + f_m(1/T_{1m}) \quad (2)$$

Comparison of the inverse of the rate constant for dissociation of the γ-CD–Tempone complex ($\sim 10^{-6}$ s^{-1})[6] to the slopes of the lines in Figure 3 (10-50 s^{-1}) demonstrates that the fast exchange limit applies, and τ_m can be neglected with respect to T_{1m}. Consequently, the slopes of the lines in Figure 3 are approximately equal to $1/T_{1m}$.

In order to verify that complexation of the CD with the nitroxide was not changing the *diamagnetic* contribution to the relaxation rates for the γ-CD–Tempone complex, the relaxation rates for a γ-CD-reduced Tempone complex (0.8:1 stoichiometry) were measured and shown to be identical within experimental error with the rates for γ-CD without Tempone (Table I).

The relationships between the paramagnetic relaxation rates in the complex and the distances between the unpaired electron and the γ-CD nuclei are given by the Solomon-Bloembergen equations. For relaxation of ^{13}C by nitroxides at 7.0 T, these equations can be simplified to[14]

$$T_1^{-1}{}_m = (C/r)^6 f(\tau_c) \quad (3)$$

where C is a constant characteristic of the paramagnetic probe and the nucleus undergoing relaxation, r is the distance between the unpaired electron and the nucleus, and $f(\tau_c)$ is the correlation function for the modulation of the dipolar interactions by motions of the complex and the Larmor frequencies of the nuclear and electron spins. If we assume that all of the nuclei in the γ-CD–Tempone complex have similar motions, which is suggested by the similar diamagnetic NT_1s for all the carbon resonances in free γ-CD and the reduced nitroxide complex, then the relative distances between the unpaired electron and the nuclei in the complex are inversely related to the sixth root of the relative nuclear relaxation rates:

$$(T_1^{-1}{}_{mi})/(T_1^{-1}{}_{mj})^{1/6} = (r_j/r_i) \quad (4)$$

The slopes of the plots of $T_1^{-1}{}_{obs}$ versus f_m (which are equal to $T_1^{-1}{}_m$) for each resonance are given in Table II, together with relative average distances $\langle r \rangle_{rel}$ between the unpaired electron density on Tempone and each ^{13}C nucleus. Carbons C3 and C5 are located closest to the unpaired electron, carbons C4 and C6 are next closest, and carbons C1 and C2 are located furthest from the unpaired electron density. If we assume a structural model for the γ-CD–Tempone complex where the unpaired electron density is centered along an axis in the middle of the hydrophobic CD cavity, these estimated distances are in qualitative agreement with the chair structure of the pyranosyl ring observed in the solid-state structures of CDs,[15] where carbons 3 and 5 are puckered toward the inside of the cavity and carbon 2 and the acetal oxygen are puckered to the outside of the cavity (see Figure 1). These distance

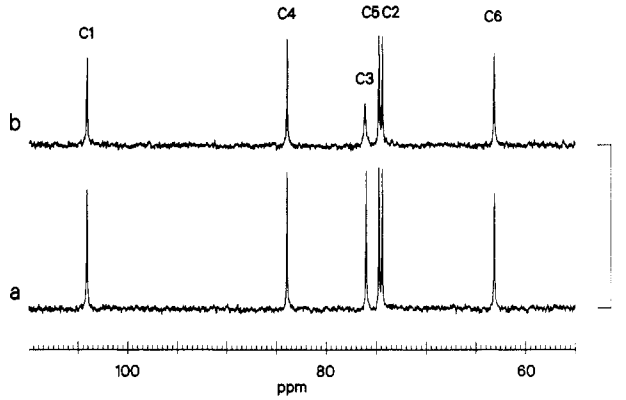

Figure 4. Proton-decoupled ^{13}C NMR spectra of (a) α-CD and (b) α-CD–DTBN inclusion complex.

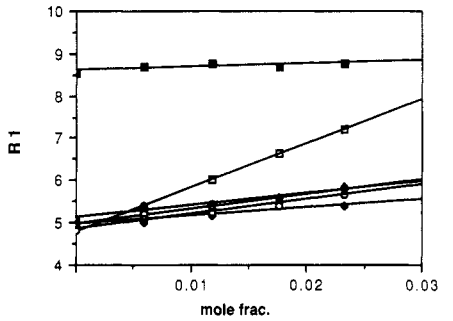

Figure 5. Effects of DTBN on the spin–lattice relaxation rates ($R1$) of carbon nuclei in α-CD. Spin–lattice relaxation rates are plotted as a function of the mole fraction of α-CD present in the α-CD–DTBN inclusion complex: (●) C1; (○) C2; (□) C3; (△) C4; (◆) C5; (■) C6.

Table III
$T_1^{-1}{}_m$ and $\langle r \rangle_{rel}$ for α-CD–DTBN Complexes

	C1	C2	C3	C4	C5	C6
$T_1^{-1}{}_m$	28.06	35.19	103.71	34.57	18.58	7.74
$\langle r \rangle_{rel}$	1.24	1.20	1.00	1.20	1.33	1.54

estimates further suggest that the unpaired electron density on Tempone penetrates significantly into the hydrophobic cavity, where it is closer to the C6 carbon than to the C1 or C2 carbons.

α-Cyclodextrin–DTBN Inclusion Complex

In order to examine the sensitivity of the relaxation rates to the structure of the inclusion complex, we examined the complex between di-*tert*-butyl nitroxide (DTBN) and α-CD. The ^{13}C spectrum of 43 mM α-CD in D_2O, pH 7.15, is shown in Figure 4a, and the spectrum in the presence of 3.7 mM DTBN is shown in Figure 4b. In contrast to the γ-CD–Tempone complex, only one carbon resonance (C3) is broadened by the nitroxide in the α-CD–DTBN complex. Plots of the spin–lattice relaxation rates for the α-CD–DTBN complex versus the mole fraction of the α-CD in the complex are shown in Figure 5. The mole fractions were calculated from K_a = 6 determined from ESR measurements.[6] If the same approximations as above are made, which are valid for this complex as well, the slopes of these lines are equal to T_{1m} for the carbon nuclei of the α-CD–DTBN complex. Values for T_{1m} and $\langle r \rangle_{rel}$ for each carbon nucleus in the α-CD–DTBN complex are given in Table III. The relative distances between the unpaired electron density on DTBN and the carbon nuclei in α-CD suggest that the penetration of the nitroxide into the hydrophobic cavity in this complex is much more limited than in the γ-CD–Tempone complex. For the α-CD–DTBN complex, carbons C1, C2, C4, and C5 are 20–30%

Figure 6. Pictoral representation of the positions of the nitroxide guests in the CD hosts.

further from the unpaired electron density than C3. Carbon 6 is more than 50% further away. These estimated distances are consistent with a structure for the complex where the nitroxide (average radius ~7 Å) is excluded from the interior of the α-CD cavity (radius ~5 Å).

A qualitative comparison of the relative distances estimated for the two complexes is instructive. If we use the X-ray and neutron diffraction crystal structures of CDs[15] as models for the positions of the glucosyl carbons, we can rank the distances between the various carbons and the top (wide end) of the hydrophobic cavity and between the various carbons and the center of the cavity of the cyclodextrin. From the top to the bottom of the cavity, the order (closest to furthest) is C3, C2 < C1, C4 < C5 < C6. From the inside to the outside of the cavity the order is C3, C5 < C4, C2, C1, C6. Ranking the relative positions of C4, C2, C1, and C6 is a difficult task because they are all very similar in distance to the center of the cavity. Comparison of these two ranking orders with the distance estimates in Tables II and III reveals that the distances between the carbons in the α-CD–DTBN complex and the unpaired electron follow (perhaps with the exception of C2) a top-down order, whereas the distances in the γ-CD–Tempone complex follow an inside-out order. The distance observed between the unpaired electron density and the C2 nucleus in the α-CD–DTBN complex can be accommodated by placing the unpaired electron at the *center* of the top of the hydrophobic cavity. The pucker of the pyranose ring makes the distance from the C2 nucleus to the center of the cavity greater than the distance from the C3 nucleus to the center.

A comparison of the variation in the estimated relative distances is also useful. The relative distances in the α-CD complex vary by ~50%, whereas the relative distances in the γ-CD complex vary by only 16%. This observation is consistent with the solid-state structures in which the relative distances of all of the carbon nuclei to the center of the cavity are more similar than the relative distances of the carbon nuclei to the top. An alternate and/or additional explanation for this observation is that the Tempone radical in the γ-CD inclusion complex is sampling multiple conformations in the cavity.

The relaxation data suggest models for the two complexes where the nitroxide in the α-CD complex is localized at the top of the hydrophobic cavity, and the nitroxide in the γ-CD complex is localized at the center of the interior of the hydrophobic cavity as shown in Figure 6. These structures are quite consistent with the sizes of the hydrophobic cavities and the nitroxide substrates and with the thermodynamics for formation of the complex. γ-CD has a cavity diameter of approximately 8.5 Å. This is slightly larger than the diameter of the Tempone substrate (~8 Å); consequently, the nitroxide is accommodated within the hydrophobic cavity, hydrophobic interactions between the guest and host are maximized, and the free energy for complex formation is large ($K_a \sim 200$). In contrast, α-CD has a cavity diameter of 5–6 Å, which is smaller than the diameter of the DTBN radical (~7 Å); consequently, the nitroxide molecule is largely excluded from the hydrophobic cavity, hydrophobic interactions are minimal, and the free energy for complex formation is relatively small ($K_a \sim 6$).

Summary

The results presented here show that (1) the ^{13}C spectra of nitroxide–CD inclusion complexes are easier to treat quantitatively than the ^{1}H spectra because they are better resolved, (2) the effects of nitroxide-induced relaxation can be used to determine a position for the unpaired spin density in the complex, (3) the structure of different complexes can be interpreted in terms of the size of the substrate relative to the size of the CD cavity and in terms of the association constant for complex formation, and (4) ESR data nicely complement the NMR measurements. Although determination of the absolute weighted average distances between the nitroxide spin density and the different carbon nuclei of the CDs in these inclusion complexes requires the determination of the correlation time, τ_c, from field-dependent relaxation measurements, the constrained nature of the CD structures allowed the positions of the nitroxide substrates to be inferred from relative measures of distances. This method may be applicable to investigations of a variety of CD inclusion complexes, including models for enzyme recognition and catalysis.

Acknowledgment. This research was supported by the donors of the Petroleum Research Fund, administered by the American Chemical Society, through a grant to M.P.E. and by the Robert A. Welch Foundation through grant to M.P.E. while he was a faculty member at the University of Texas at El Paso. This work was performed under the auspices of the United States Department of Energy.

Registry No. α-CD, 10016-20-3; α-CD–DTNB, 122470-82-0; β-CD, 7585-39-9; γ-CD, 17465-86-0; tempone–γ-CD complex, 105613-47-6.

References and Notes

(1) Abbreviations: CD, cyclodextrin; α-CD is a CD with six glucosyl residues; β-CD and γ-CD have seven and eight glucosyl residues, respectively; Tempone, 2,2,6,6-tetramethyl-4-oxopiperidinyl-1-oxy; DTBN, di-*tert*-butyl nitroxide; TSP, 4,4-dimethyl-4-silapentane-1-sulfonate; NT_1, the ^{13}C spin–lattice relaxation time normalized for the number of attached protons by multiplying the observed T_1 by the number of directly bonded protons; COSY, correlated spectroscopy.
(2) Saenger, W. *Angew. Chem., Int. Ed. Engl.* **1980**, *19*, 344–362. Bender, M. L.; and Komiyama, M. *Cyclodextrin Chemistry*; Springer-Verlag: New York, 1978.
(3) Tabushi, I. *Acc. Chem. Res.* **1982**, *15*, 66–72.
(4) Hinze, W. *Sep. Purif. Methods* **1981**, *10*, 159. Chang, C. A., Wu, Q.; Armstrong, D. *J. Chromatogr.* **1985**, 354–454.
(5) Behr, J. P.; Lehn, J. M. *J. Am. Chem. Soc.* **1976**, *98* 1743–1747. Hall, L.; Lim, T. *J. Am. Chem. Soc.* **1984**, *106*, 1858–1859. Martinie, J.; Michon, J.; Rassat, A. *J. Am. Chem. Soc.* **1975**, *97*, 1818. Okazaki, M.; Kuwata, K. *J. Phys. Chem.* **1985**, *89*, 4437. Flohr, K.; Paton, R.; Kaiser, E. *J. Am. Chem. Soc.* **1975**, *97*, 1209.
(6) Eastman, M. P.; Freiha, B.; Hsu, C.; Lum, K.; Chang, C. A. *J. Phys. Chem.* **1987**, *91*, 1953. Eastman, M. P.; Freiha, B.; Hsu, C.; Chang, C. A. *J. Phys. Chem.* **1988**, *92*, 11682.
(7) Inoue, Y.; Hoshi, H.; Sakuri, M.; Chujo, R. *J. Am. Chem. Soc.* **1985**, *107*, 2319–2323. Beregon, R. J.; Channing, M. A.; McGovern, K. *J. Am. Chem. Soc.* **1978**, *100*, 2878.
(8) Mildvan, A. S.; Cohn, M.; Leigh, J. S., Jr. In *Magnetic Resonance in Biological Systems*; Ehrenberg, A., Malmstrom, B. G., Vanngard, T., Eds.; Pergamon: Oxford, 1967; p 133. Mildvan, A. S.; Leigh, J. S., Jr.; Cohn, M. *Biochemistry* **1967**, *6*, 1895.
(9) Ohara, M.; Kobayashi, G. *Nippon Kagaku Kaishi* **1983**, *2*, 300–302. Ohara, M.; Fukada, J. *Carbohydr. Res.* **1982**, *105*, 154.
(10) Fung, C. H.; Gupta, R. K.; Mildvan, A. S. *Biochemistry* **1976**, *15*, 85. London, R. E.; Groff, J. P.; Cocco, L.; Blakley, R. L. *Biochemistry* **1982**, *21*, 4450.
(11) DISNMR Software, version DISN85, Bruker Instruments, Billerica, MA 01821.

(12) Colson, P.; Jennings, H. J.; Smith, I. C. P. *J. Am. Chem. Soc.* **1974**, *96*, 8081. Beragon, R. J.; Channing, M. A.; Gibeily, G. J.; Pillor, D. M. *J. Am. Chem. Soc.* **1977**, *99*, 5146.
(13) Aue, W. P.; Bartholdi, E.; Ernst, R. R. *J. Chem. Phys.* **1976**, *64*, 2229.
(14) Mildvan, A. S.; Gupta, R. K. *Methods Enzymol.* **1978**, *49G*, 322-359. Swift, T. J.; Connick, R. E. *J. Chem. Phys.* **1962**, *37*, 307. Bertini, I.; Luchinat, C. *NMR of Paramagnetic Molecules in Biological Systems*; Benjamin Cummings: Menlo Park, 1986.
(15) MacLennan, J. M.; Stezowski, J. J. *Biochem. Biophys. Res. Commun.* **1980**, *92*, 929-932. Chacko, K. K.; Saenger, W. *J. Am. Chem. Soc.* **1981**, *103*, 1708-1715. Zabel, V.; Saenger, W.; Mason, S. A. *J. Am. Chem. Soc.* **1986**, *108*, 3664-3673.

Effect of Hydration on Conformational Change or Stabilization of (1→3)-β-D-Glucans of Various Chain Lengths in the Solid State As Studied by High-Resolution Solid-State ^{13}C NMR Spectroscopy

Hazime Saitô,*,† Motoko Yokoi,† and Yuko Yoshioka‡

Biophysics Division and Chemotherapy Division, National Cancer Center Research Institute, Tsukiji 5-Chome, Chuo-ku, Tokyo, Japan 104. *Received December 21, 1988; Revised Manuscript Received March 17, 1989*

ABSTRACT: ^{13}C NMR spectra of hydrated (1→3)-β-D-glucans from various sources were recorded after equilibrating samples in an atmosphere of 96% relative humidity in a desiccator over 8 h to gain insight into hydration-induced conformational change or stabilization. It was found that the effect of hydration depends strongly on the initial conformation of the glucans studied. The ^{13}C NMR peaks of curdlan hydrate ($\overline{DP}_n$ 540) were substantially displaced (up to 2.5 ppm) from those of curdlan powder (form II) owing to hydration-induced conformational change as an intermediate step to form the triple helix. The resultant conformation (form II′) turned out to be the same as the single-helical portion of the elastic gel because the ^{13}C chemical shifts of both states were identical within an error of ±0.1 ppm. Hydration, however, did not induce any significant displacement of peaks for either glucans of low molecular weight ($DP_n \leq 38$) or annealed curdlan, adopting form I (oligomer type) or form III (triple helix), respectively, but narrowed all spectral peaks except for those of laminariheptaose. The peak narrowing is explained by distorted or interrupted conformations of the anhydrous state readjusting on hydration. It is now clear that the presence of a hydration-induced single-helical conformation is an essential condition for gel-forming ability in linear (1→3)-β-D-glucans. Finally, the hydration-induced spectral change of paramylon is discussed.

Introduction

It is well recognized that a variety of physical properties of (1→3)-β-D-glucans such as density, crystallinity, solubility, gel-forming ability, etc., vary with the degree of polymerization and extent of branching, which depend on the source and history of the samples.[1-3] A linear (1→3)-β-D-glucan of high molecular weight, curdlan ($\overline{DP}_n$ 540), is known to form an elastic gel when its aqueous suspension is heated above 54 °C.[1] From a study of acid-degraded glucans, linear glucans with number-average degree of polymerization (DP_n) > 20 were found to be insoluble in aqueous media,[4] whereas branched glucans are soluble irrespective of their chain lengths.[4,5] These physical properties are related to secondary or tertiary structures of individual chains, molecular assembly, or aggregation and consequently to their biological function as structural components in cell walls or as reserve polysaccharides in bacteria, algae, fungi, or plants. In addition, it has been proposed that such physical properties are closely related to their specific activity as biological response modifiers (BRM), including antitumor activity.[6-9]

Previous solid-state ^{13}C NMR studies[2,3,11-13] showed that the existence of three types of conformations,[14] form I (lower molecular weight oligomers), form II (single chain), and form III (triple helix), are distinguishable in linear and branched (1→3)-β-D-glucans by examination of the conformation-dependent displacements of the C-3 ^{13}C NMR peak[17-19] at the glycosidic linkages as well as a peak profile of C-2, C-4, and C-5 carbons among several types of samples used (Table I). Conformational characterization by X-ray diffraction[20-22] is feasible only for form III samples, as the others are noncrystalline. Further, we found that any attempt to achieve better crystallinity resulted in conformational changes, as judged by the ^{13}C NMR pattern.[2,3] In this connection, conformational characterization by ^{13}C NMR is indispensable for interpretation of the physical properties of (1→3)-β-D-glucans as a complementary means of X-ray diffraction study.

Hydration has been recognized as a very important process in conformational stabilization of a variety of biological macromolecules. Previous ^{13}C NMR studies[23-25] have demonstrated that hydration of amylose, starches, or silk fibroins caused either substantial narrowing or displacements of ^{13}C NMR peaks as a result of conformational stabilization or change, respectively, depending on the types of molecular structures. Hydration/dehydration processes will induce conformational changes if water molecules are involved at chain positions of crucial importance in maintaining a secondary structure. As for (1→3)-β-D-glucans, it has been shown that hydration induces substantial spectral changes in curdlan and paramylon,[26,27] although the resulting conformations have not yet been clarified. In particular, Stipanovic and Giammatteo demonstrated that the three conformations "anhydrous", "hydrate", and "swollen" are distinguishable by solid-state ^{13}C NMR spectra.[27,28]

In this connection, it seems to be very important to reveal which types of initial conformations are susceptible

† Biophysics Division.
‡ Chemotherapy Division.

0024-9297/89/2222-3892$01.50/0